

# The Effects of Short-Term Light Adaptation on the Human Post-Illumination Pupil Response

Daniel S. Joyce,<sup>1,2</sup> Beatrix Feigl,<sup>1,3,4</sup> and Andrew J. Zele<sup>1,2</sup>

<sup>1</sup>Institute of Health and Biomedical Innovation, Queensland University of Technology (QUT), Brisbane, Australia

<sup>2</sup>Visual Science Laboratory, School of Optometry and Vision Science, Queensland University of Technology (QUT), Brisbane, Australia

<sup>3</sup>Medical Retina Laboratory, School of Biomedical Sciences, Queensland University of Technology (QUT), Brisbane, Australia

<sup>4</sup>Queensland Eye Institute, Brisbane, Australia

Correspondence: Andrew J. Zele, Visual Science Laboratory, Institute of Health and Biomedical Innovation, 60 Musk Avenue, Kelvin Grove, Queensland 4059, Australia; [andrew.zele@qut.edu.au](mailto:andrew.zele@qut.edu.au).

Submitted: May 15, 2016

Accepted: September 2, 2016

Citation: Joyce DS, Feigl B, Zele AJ. The effects of short-term light adaptation on the human post-illumination pupil response. *Invest Ophthalmol Vis Sci.* 2016;57:5672-5680. DOI:10.1167/iovs.16-19934

**PURPOSE.** We determine the effect of short-term light adaptation on the pupil light reflex and the melanopsin mediated post-illumination pupil response (PIPR). Inner and outer retinal photoreceptor contributions to the dark-adapted pupil response were estimated.

**METHODS.** In Experiment A, light adaptation was studied using short wavelength lights ranging from subthreshold to suprathreshold irradiances for melanopsin signaling that were presented before (5–60 seconds) and after (30 seconds) a melanopsin-exciting stimulus pulse. We quantified the pupil constriction and the poststimulus response amplitudes during dark (PIPR) and light (poststimulus pupil response, PSPR) adaptation. In Experiment B, colored prestimulus adapting lights were univariant for melanopsin or rod excitation.

**RESULTS.** Increasing the prestimulus duration and irradiance of adapting lights increased the pupil constriction amplitude when normalized to the dark-adapted baseline but reduced its amplitude when normalized to the light-adapted baseline. Light adaptation at irradiances suprathreshold for melanopsin activation increased the PIPR amplitude, with larger changes at longer adaptation durations, whereas the PSPR amplitude became more attenuated with increasing irradiances, independent of duration. Rod versus melanopsin univariant adaptation did not alter the constriction amplitude but increased the PIPR amplitude in the rod condition. Correlations between millimeter pupil constriction and PIPR amplitudes were eliminated when normalized to the baseline diameter.

**CONCLUSIONS.** The findings have implications for standardizing light adaptation paradigms and the choice of pupil metrics in both laboratory and clinical settings. Light and dark adaptation have opposite effects on the pupil metrics, which should be normalized to baseline to minimize significant correlations between constriction and PIPR amplitudes.

Keywords: pupil, melanopsin, adaptation

Intrinsically photosensitive retinal ganglion cells (ipRGC) project to over a dozen brain regions<sup>1–8</sup> including the olivary pretectal nucleus (OPN), which controls the pupil response.<sup>9</sup> Intrinsically photosensitive RGCs receive extrinsic synaptic inputs from outer retinal rod and cone photoreceptors, as well as signal intrinsically via the photopigment melanopsin.<sup>3,10,11</sup> The pupil light reflex (PLR) therefore provides an objective and noninvasive measure of the functional correlates of both extrinsic and intrinsic ipRGC signaling in humans. Under dark-adapted conditions it is known that ipRGCs primarily control the post-illumination pupil response (PIPR) in humans<sup>12–14</sup> and nonhuman primates<sup>14</sup> from at least 1.7 seconds post-illumination,<sup>15</sup> because the PIPR spectral sensitivity matches that of the melanopsin nomogram.<sup>3,15</sup> It is largely unknown how light adaptation affects the PIPR amplitude.

Light adaptation alters the steady-state pupil constriction: The constriction amplitude increases when assessed 40 minutes after a 5 minute pre-exposure to long wavelength light with low-melanopsin excitation.<sup>16</sup> Preadaptation to 30 seconds of short- or long-wavelength light also increases the subsequent steady-state pupil constriction amplitude to a blue-

stimulus light with high-melanopsin excitation.<sup>17</sup> Preadaptation for 10 minutes to photopic broadband light (30 cd.m<sup>-2</sup>) attenuates the PIPR amplitude measured in the dark in response to a melanopsin-exciting stimulus pulse, with the PIPR gradually recovering and plateauing 20-minutes postadaptation.<sup>18</sup> Studies have demonstrated complete attenuation of the PIPR amplitude during continuous adaptation to blue light designed to desensitize rods,<sup>19,20</sup> but the causal mechanism for this attenuation is unknown and may be due to incomplete melanopsin adaptation given that the PIPR mainly reflects melanopsin signaling,<sup>12–15</sup> at least under dark-adapted conditions.

We propose that light adaptation may affect the PIPR amplitude due to the different temporal dynamics and light adaptation characteristics of the extrinsic and intrinsic ipRGC pathways as observed in electrophysiological recordings.<sup>3,21–23</sup> We systematically examine how light adaptation affects the pupil constriction amplitude (reflecting both extrinsic + intrinsic ipRGC contributions) and the PIPR amplitude (reflecting intrinsic ipRGC contributions) by altering the duration and irradiance of a short-wavelength adapting field

presented pre- and poststimulus to a pulse with high-melanopsin excitation (Experiment A). Because steady-state pupil control is dominated by the activity of extrinsic rod and intrinsic melanopsin contributions,<sup>24</sup> we determined how the constriction and PIPR amplitudes are altered by fixing the excitations of these photoreceptor classes (Experiment B).

## METHODS

### Participants

Experiment A included two participants (1 male age 33 and 1 female age 40) and Experiment B included four males (mean age 31.8, SD 0.5). Ophthalmologic examination (slit-lamp examination, IOP with tonometry [Icare, Vantaa, Finland], ophthalmoscopy, color vision [desaturated Lanthony D15] and optical coherence tomography [OCT; Cirrus HD-OCT; Carl Zeiss Meditec, Dublin, CA, USA]) confirmed all participants had normal eye health. Participants had a best-corrected visual acuity of 6/6 or greater (Bailey Lovie chart). The University's Human Research Ethics Committee (ethics number 1400000842) approved the experiment, which was conducted in accordance with the Code of Ethics of the World Medical Association (Declaration of Helsinki). Informed consent was obtained from participants before the experiment began.

### Apparatus

Pupillometry stimuli were generated using a custom-built Maxwellian-view optical system with three light-emitting diode primary lights (5 mm; 'blue'  $\lambda_{\max}$  464 nm, full width at half maximum (FWHM); 26 nm, 'cyan'  $\lambda_{\max}$  512 nm, FWHM 32 nm; and 'green'  $\lambda_{\max}$  560 nm, FWHM 12 nm; measured with a StellarNet EPC200C spectroradiometer, Tampa, FL, USA). The light from the primaries was spatially homogenized with 5° light shaping diffusers (Physical Optics Corp., Torrance, CA, USA) then focused through achromat doublet lenses (Edmund Optics, Barrington, NJ, USA). Each primary light was aligned along the optical axis using 50:50 beam splitters and field size was controlled by an aperture to create a 36° field. A 100-mm Fresnel lens (Edmund Optics, Singapore) projected stimuli into the plane of the right pupil in Maxwellian-view. Adapting field and stimulus irradiances were controlled by custom coded software (Xcode 3.3.3.5, Apple, Inc., Cupertino, CA, USA) and calibrated neutral density filters (Ealing, Natick, MA, USA). A chin rest and temple bars maintained participant alignment. The participant's left eye was recorded under infrared illumination ( $\lambda_{\max}$  851 nm) in monochrome at 60 Hz (640 × 480 pixels; Point Grey FMVU-03MTM-CS; Richmond, BC, Canada; Computar TEC55 55 mm telecentric lens; Computar, Cary, NC, USA); recordings were synchronized to begin at paradigm onset and pupil diameters were analyzed offline using a custom developed program coded in Xcode.

### Experimental Design

Experiment A determined if the adapting field duration (5–60 second prestimulus onset) and irradiance (10.5–13.5 log photons.cm<sup>-2</sup>.s<sup>-1</sup>) systematically altered the PIPR amplitude in response to a 1-second blue stimulus pulse with high melanopsin excitation ( $\lambda_{\max}$  464 nm, 15.1 log photons.cm<sup>-2</sup>.s<sup>-1</sup>). Pre-exposure durations were selected based upon the long latencies to peak signaling and long integration times of melanopsin compared to outer retinal photoreceptors,<sup>3,22,23</sup> and adapting irradiances spanned a range from below to above threshold for measured melanopsin contributions to the human PIPR.<sup>13,14</sup> To evaluate the alternative hypothesis that the observed PIPR attenuation could be an artefact of

normalizing the data to the baseline (light adapted) pupil diameter, rather than to its dark-adapted baseline, we analyze the pupil metrics normalized to both the dark and light adapted baseline diameters (see the Analyses section). The paradigm for Experiment A consisted of a 10-second dark-adapted baseline, 5 to 60 seconds prestimulus light adaptation, the 1-second stimulus pulse, 30 seconds of continued light adaptation, and a 40 second PIPR measured after offset of the adapting field (see schematic in Fig. 1A). Three repeats of each condition were obtained for two observers.

To examine interactions between extrinsic and intrinsic signal contributions to the pupil light reflex, Experiment B investigated the dark adapted pupil constriction and PIPR amplitudes after exposure to prestimulus adapting fields that altered the (1) color (blue, cyan, green), (2) duration (1, 3, 5 seconds), (3) irradiance (10.5, 11.5, 12.5, 13.5 log photons.cm<sup>-2</sup>.s<sup>-1</sup>, but see next paragraph), and (4) photoreceptor univariance (melanopsin, rods) of the adapting fields.

Adapting field durations and irradiances were selected based upon the physiological temporal signaling characteristics (latency and time to peak) of the extrinsic and intrinsic ipRGC pathways,<sup>3,4,21–23</sup> spanning the mesopic to photopic light levels of their signaling range.<sup>3,21</sup> For each colored field, the light levels were specified relative to the peak spectral sensitivity of melanopsin or rods for the four irradiances; therefore, these irradiances as expressed are indicative only and will underestimate the true irradiance of each field as none of the primaries had a  $\lambda_{\max}$  of 482 or 507 nm. The green 13.5 log photons.cm<sup>-2</sup>.s<sup>-1</sup> condition was not generated because of the low peak irradiance output of the green primary.

Melanopsin or rod univariance was maintained across the three adapting field wavelengths by adjusting the irradiance of each blue, cyan, and green primary light based upon the spectral profile of each primary in conjunction with the known spectral sensitivities of melanopsin inputs to the PIPR ( $\lambda_{\max}$  482 nm<sup>12–14,25</sup> and rod inputs to image forming vision ( $\lambda_{\max}$  507 nm<sup>26</sup>), based upon the principle of univariance,<sup>27,28</sup> whereby photoreceptor spectral sensitivity specifies the probabilistic photon catch as a function of wavelength.

A schematic of the protocol for a single repeat is shown in Figure 1B. Each repeat consisted of a baseline period (5, 7, or 9 seconds) prior to onset of the prestimulus field (5, 3, or 1 seconds) so that the combined baseline and prestimulus field duration was always 10 seconds. This was followed by a 1-second blue stimulus pulse (15.1 log photons.cm<sup>-2</sup>.s<sup>-1</sup>) as used in Experiment A, and a poststimulus period of 40 seconds. Three identical repeats of 51 seconds in duration were presented successively (153-seconds total time) to form a triplicate, and each triplicate was presented twice per observer for a total of six repeats per observer. Triplicate presentations were randomly ordered.

### Procedure

Participants were aligned in the pupilometer (undilated) in Maxwellian-view and then dark adapted for 7 minutes prior to the pupil recordings. Head position was maintained with a supraorbital arch stabilizer, temple bars, and chin rest. After each triplicate measurement, the participant removed their head from the pupilometer, remained seated and dark adapted for 7 minutes until the after-image had dissipated and the pupil had returned to baseline.<sup>15</sup> Recordings were conducted in the morning or afternoon to avoid circadian attenuation of the PIPR that occurs in the evening prior to melatonin onset.<sup>29</sup> Each experimental session lasted approximately 1 hour, and participants volunteered approximately 8 hours of their time in Experiment A and approximately 23 hours of their time in Experiment B.

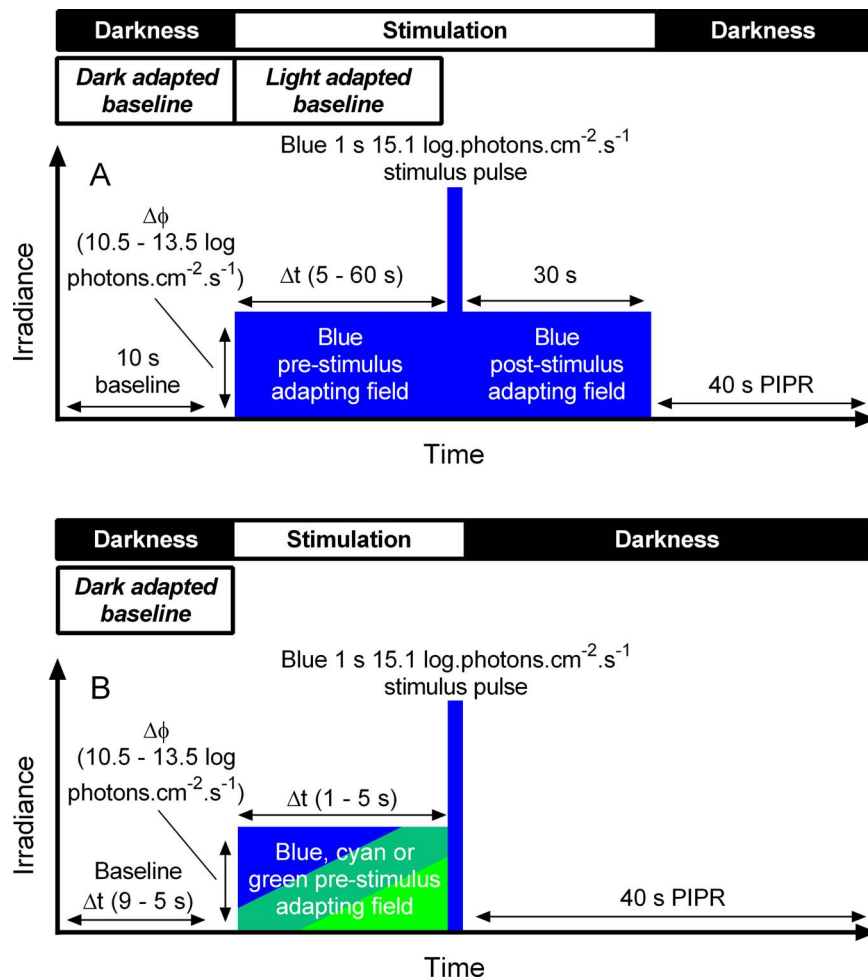


**FIGURE 1.** Schematic of the experimental paradigms. The duration and irradiance of a blue-adapting field presented prestimulus that continues for 30 seconds after stimulus offset was modified in Experiment A (A). We also alter the photoreceptor univariance, color, duration, and irradiance of an adapting field presented prestimulus only in Experiment B (B).

## Analyses

Analyses were performed offline, and each tracing was visualized for the manual removal of blink artefacts, which were linearly interpolated (MATLAB R2014a 8.3.0.532; MathWorks, Natick, MA, USA). In Experiment A, dark-adapted and light-adapted pupil metrics were derived from each tracing: the dark adapted metrics consisted of the maximum constriction amplitude and PIPR (measured 6 seconds after the poststimulus adapting field ceased<sup>13,20</sup>) normalized to the dark-adapted baseline diameter. The light-adapted metrics consisted of the maximum constriction amplitude and 6 seconds poststimulus pupil response (designated the PSPR: analogous to the PIPR, but measured 6 seconds after the stimulus pulse while the adapting field was still on) normalized to the light-adapted baseline. The relationships between the pupil metrics and adapting field irradiances for each duration were modelled using 4-parameter (variable slope) log dose-response curves (GraphPad Prism 6.07; GraphPad, La Jolla, CA, USA), in accordance with the log dose-response relationship between irradiance and PIPR amplitude.<sup>14</sup>

In Experiment B, each of the six repeats (see Experimental Design section) were initially visualized with box plots (not shown) to confirm that there were no systematic order effects upon the constriction and PIPR amplitudes, and the results averaged. Extrinsic and intrinsic ipRGC contributions to the

pupil light reflex were assessed by measuring the maximum constriction amplitude,<sup>30</sup> while the intrinsic melanopsin contribution was assessed by the post-illumination pupil response at 6 seconds after stimulus offset.<sup>13,20</sup> Generalized estimating equations (IBM SPSS Statistics 21; IBM, Armonk, NY, USA) were used to determine the influence of adapting field univariance (melanopsin or rod), color, duration, and irradiance upon constriction and PIPR amplitudes. This quasiparametric method is robust to violations of normality and was used to apply a linear model, which accounted for clustering within persons. Univariate models were initially generated for each of the four variables, and significant variables ( $P < 0.05$ ) were entered into the composite model stepwise in order of increasing  $P$  value to assess their impact on the model fit. To determine if prestimulus fields altered the variability of the PLR, coefficients of variation (CVs) were calculated for each metric.

## RESULTS

The effect of prestimulus adapting field irradiance and duration upon the pupil response were measured, and representative pupil tracings from Experiment A are shown in Figures 2A and 2D. These traces highlight the primary pupil events, including baseline, prestimulus adapting field onset, stimulus pulse onset, poststimulus field onset, and adapting field offset. When

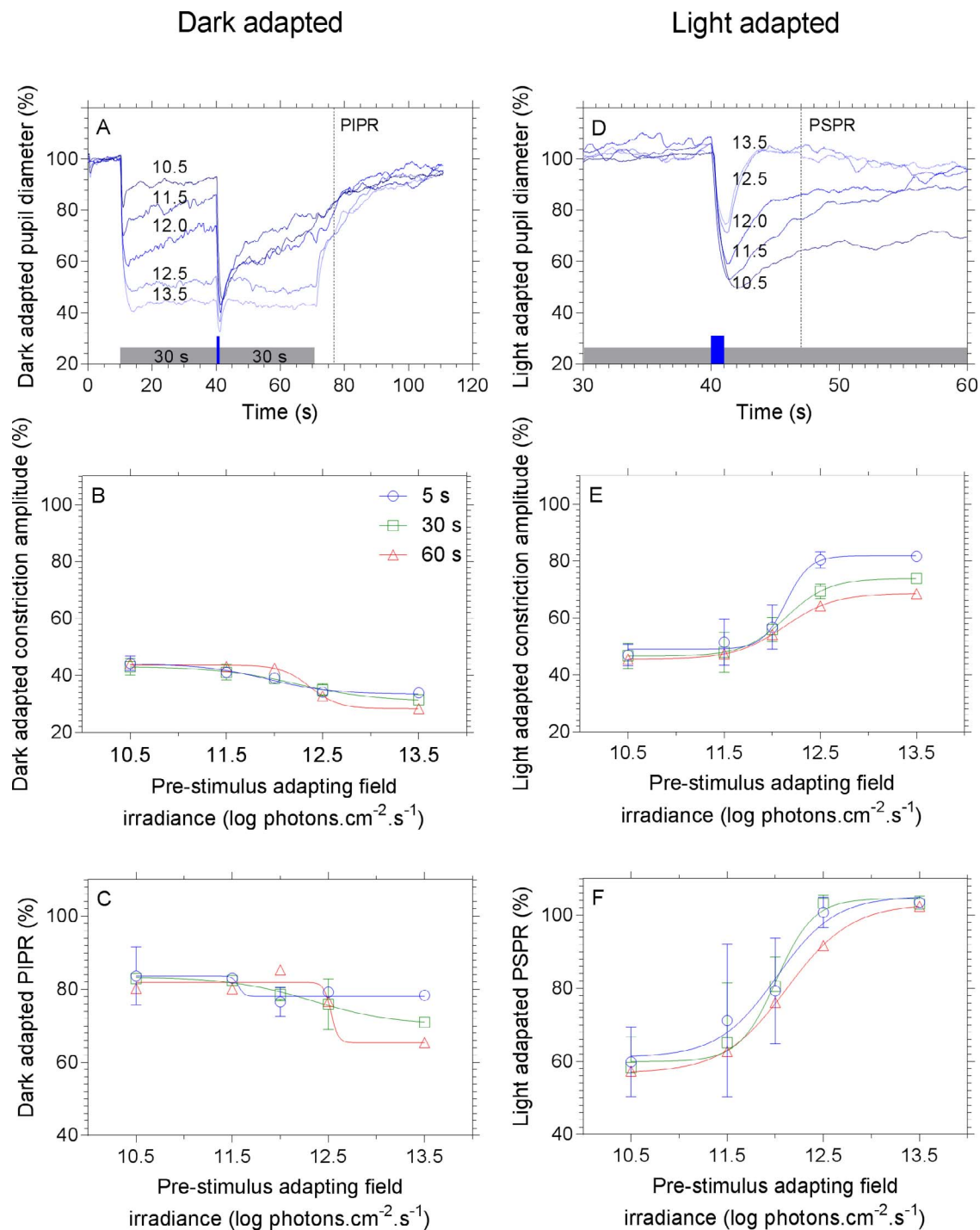


**FIGURE 2.** Dark- and light-adapted normalized pupil tracings and metrics. Representative example tracings for a single observer for the 30-second prestimulus adaptation condition are shown (A, D). The traces are normalized to the dark-adapted baselines (A) or the light-adapted baselines (D). The blue-adapting field was followed by a 1 second  $15.1 \log \text{photons.cm}^{-2}.\text{s}^{-1}$  blue ( $\lambda_{\text{max}} 464 \text{ nm}$ ) stimulus pulse and 30-second poststimulus field (blue bar positioned at 40 seconds). Prestimulus irradiances ( $\log \text{photons.cm}^{-2}.\text{s}^{-1}$ ) and durations are inset in the panels. Dashed vertical lines indicate the timing of the PIPR (A) and PSPR (D) measurements. The tracings show the average of three repeats for each condition. The mean constriction amplitude data for all irradiance and duration combinations are shown normalized to dark- (B) and light- (E) adapted baselines as well as the dark-adapted PIPR (C) and light-adapted PSPR (F). Error bars represent SDs.

normalized to the dark-adapted baseline (Fig. 2A), the mean data show that increasing the adapting field irradiance increases the constriction (Fig. 2B) and PIPR amplitudes (Fig. 2C). In contrast, when the same data are referenced to the light-adapted baseline (Fig. 2D), increasing irradiance decreases the constriction (Fig. 2E) and PSPR (Fig. 2F) amplitudes at

irradiance that are suprathreshold for melanopsin signalling. For suprathreshold irradiances, there is an increase in the dark-adapted constriction and PIPR amplitudes (Figs. 2B, 2C, respectively) as well as in the light-adapted constriction and PSPR amplitudes (Figs. 2E, 2F, respectively) with increasing prestimulus adapting field duration.

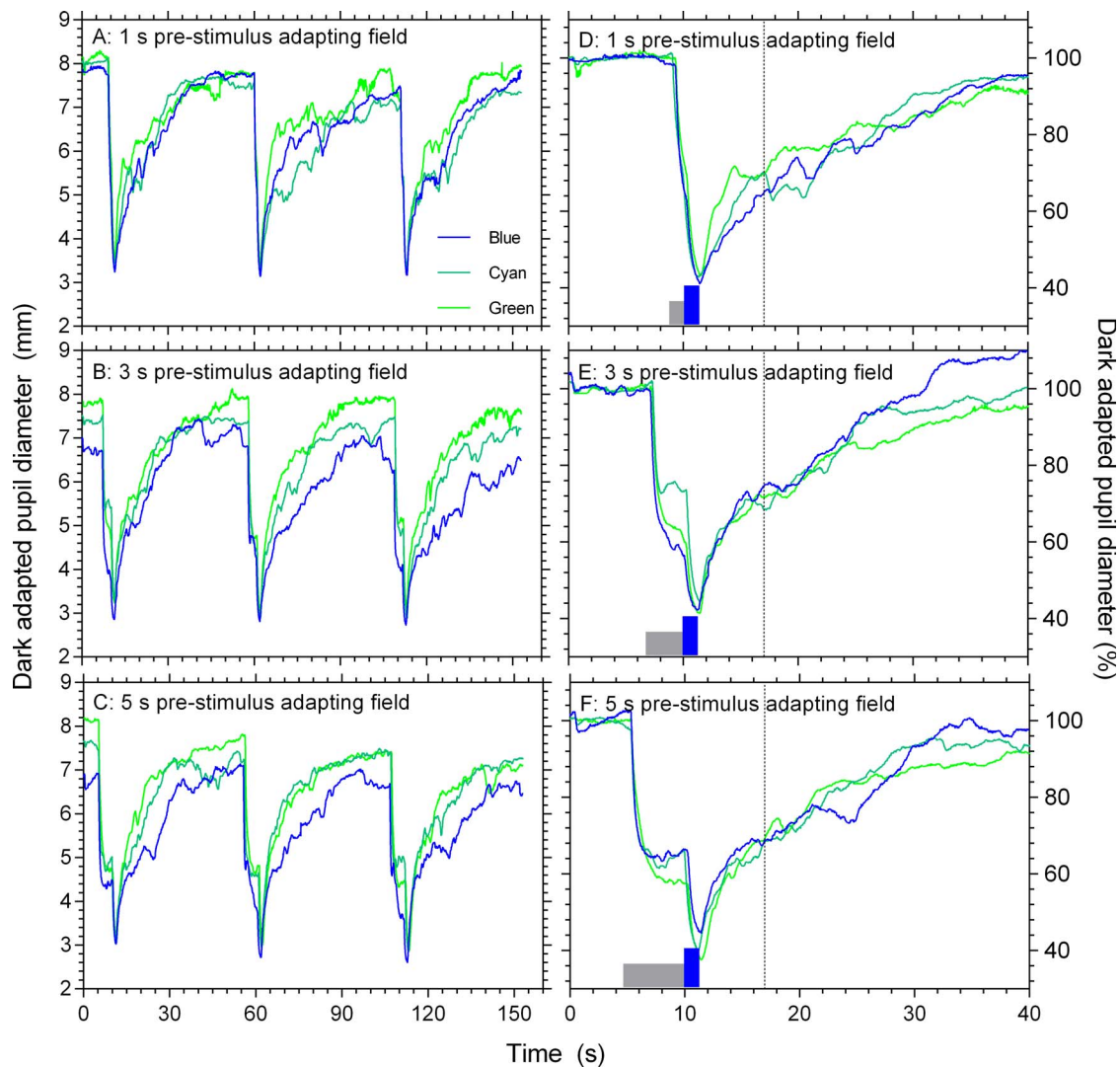


**FIGURE 3.** Example triplicate pupil tracings from a single participant. Each triplicate consists of three repeats (A–C), each triplicate was presented twice and the data from all six repeats were averaged to derive percentage constriction and PIPR amplitudes. (D–F) The first repeat expressed relative to baseline. Data are from the  $\sim 10.5 \log \text{photons} \cdot \text{cm}^{-2} \cdot \text{s}^{-1}$  melanopsin field condition. In each condition, the adapting field (durations and colors inset, gray boxes in right panel) is followed immediately by a 1-second blue  $15.1 \log \text{photons} \cdot \text{cm}^{-2} \cdot \text{s}^{-1}$  stimulus pulse with high melanopsin excitation. Vertical dashed lines indicate the PIPR measurement time.

Figures 3A through 3C (left panels) show example triplicate pupil tracings from Experiment B and demonstrate the initial constriction event in response to the preadaptation light followed by the constriction in response to the stimulus pulse (Figs. 3D–F, right panels). Typically, pupil metrics are reported in either absolute millimeter units<sup>14,24,31</sup> or normalized to baseline,<sup>15,20,30,32,33</sup> with the assumption of the independence of these metrics from each other as well as pupil baseline. However, Experiment A demonstrated that light adaptation influences the amplitude of pupil metrics derived from the PLR. We therefore determined the relationships between the dark adapted (absolute) millimeter baseline pupil diameter, constriction, and PIPR amplitudes when expressed in millimeters (Fig. 4A) or normalized to the dark-adapted baseline pupil diameter (Fig. 4B). When expressed in millimeters, both pupil metrics are dependent upon the amplitude of the dark-adapted pupil diameter measured prior to onset of the adapting fields, such that increasing baseline diameter predicts increasing response magnitude (Fig. 4A). The correlations are high between baseline diameter and constriction amplitude ( $r = .653$ ,  $P < 0.001$ ), baseline diameter and PIPR amplitude ( $r =$

$.827$ ,  $P < 0.001$ ), and constriction amplitude and PIPR diameter ( $r = .598$ ,  $P < 0.001$ ), indicating that constriction amplitude can account for 36% of the variance in PIPR amplitude.

When the metrics are normalized to the baseline and expressed as a percentage, millimeter baseline size does not predict PIPR amplitude but does predict the minimum amplitude (Fig. 4B). The data indicate that increasing baseline diameter by a millimeter increases the normalized constriction amplitude by 7.35%. Expressing the metrics in percentage baseline units nullifies the correlation between baseline diameter and constriction amplitude ( $r = .035$ ,  $P = 0.576$ ) and baseline diameter and PIPR amplitude ( $r = -.038$ ,  $P = 0.539$ ), and weakens the correlation between constriction amplitude and PIPR ( $r = .169$ ,  $P = 0.006$ ), such that constriction amplitude accounts for less than 3% of the variation in PIPR amplitude.

Generalized estimating equations were used to determine the dependence of the pupil metrics on the color, duration, irradiance, and univariance of the prestimulus adapting fields (Fig. 5). For constriction amplitude, the final model specified

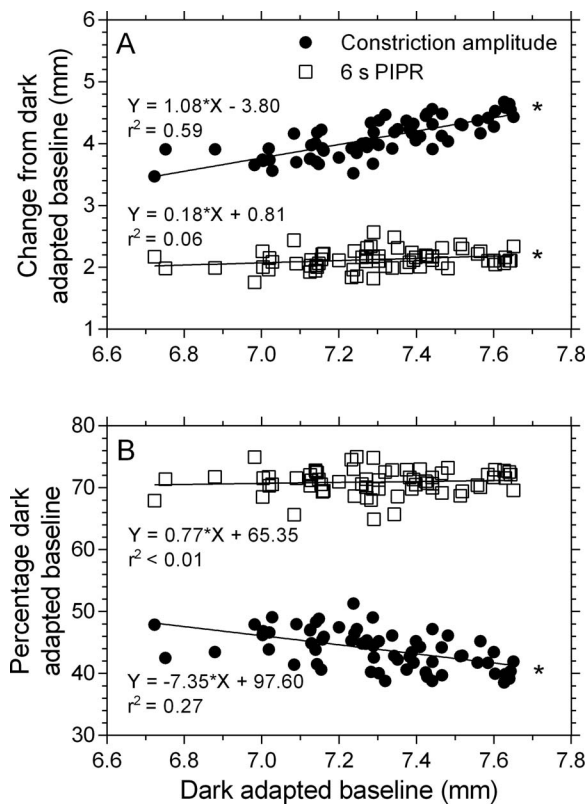


**FIGURE 4.** Dependence of the pupil light reflex metrics on pupil baseline diameter. Mean data is expressed as absolute change from baseline (A) and normalized baseline (B). Data are derived from all preadapting photoreceptor univariates, durations, irradiances, and colors. The *asterisk* denotes that the slope significantly differs from 0.

an effect of duration ( $P < 0.001$ ) and irradiance ( $P < 0.001$ ). Therefore, melanopsin and rod univariant background fields did not differentially affect constriction amplitude (Fig. 5A) with group means of 43.91% (SD 4.93) and 43.74% (SD 4.37), respectively. Similarly, blue, cyan, and green backgrounds (Fig. 5B) had no effect on constriction amplitude with means of 43.56% (SD 4.37), 44.14% (SD 4.60), and 43.75% (SD 5.09), respectively. As seen in Figure 5C, there was a trend evident that increasing background field duration increased constriction amplitude (1 second: 46.65% SD 4.14; 3 seconds: 42.58% SD 4.30; 5 seconds: 42.24% SD 4.19) for both the melanopsin and rod data such that a 1-second increase in adapting field duration increased constriction amplitude by 1.37% (95% confidence interval [CI] 1.20–1.54). Constriction amplitude trended to increase with increasing relative irradiance (Fig. 5D;  $\sim 10.5 \log \cdot \text{photons} \cdot \text{cm}^{-2} \cdot \text{s}^{-1}$ : 45.55% SD 5.09,  $\sim 11.5 \log \cdot \text{photons} \cdot \text{cm}^{-2} \cdot \text{s}^{-1}$ : 44.51% SD 4.22,  $\sim 12.5 \log \cdot \text{photons} \cdot \text{cm}^{-2} \cdot \text{s}^{-1}$ : 43.01% SD 4.09,  $\sim 13.5 \log \cdot \text{photons} \cdot \text{cm}^{-2} \cdot \text{s}^{-1}$ : 41.44% SD 4.18) for both the melanopsin and rod conditions, a 1-log unit increase in adapting field irradiance increased constriction amplitude by 1.10% (95% CI 0.91–1.29).

For the PIPR amplitude, the final generalized estimating equation model specified an effect of photoreceptor univariance ( $P = 0.011$ ) and irradiance ( $P = 0.002$ ). Mean PIPR amplitude was 1.69% (95% CI 0.38–3.00) less sustained for melanopsin univariant adapting fields (71.81% SD 3.44) compared with rod univariant fields (70.12% SD 3.76, Fig. 5E). Background color did not influence PIPR amplitude (Fig. 5F; blue: 71.07% SD 2.92, cyan: 71.52% SD 3.78, green: 70.08% SD 4.34) nor did adapting field duration (Fig. 5G; 1

second: 71.59% SD 3.68, 3 seconds: 70.35% SD 3.57, 5 seconds: 70.95% SD 3.77). The PIPR amplitude trended to be less sustained as the relative irradiance of the adapting field increased (Fig. 5H;  $\sim 10.5 \log \cdot \text{photons} \cdot \text{cm}^{-2} \cdot \text{s}^{-1}$ : 69.79% SD 3.47;  $\sim 11.5 \log \cdot \text{photons} \cdot \text{cm}^{-2} \cdot \text{s}^{-1}$ : 71.19% SD 4.29;  $\sim 12.5 \log \cdot \text{photons} \cdot \text{cm}^{-2} \cdot \text{s}^{-1}$ : 70.93% SD 3.25;  $\sim 13.5 \log \cdot \text{photons} \cdot \text{cm}^{-2} \cdot \text{s}^{-1}$ : 72.44% SD 3.18, such that a 1 log unit increase in adapting field irradiance reduced the magnitude of the PIPR by 0.74% (95% CI 0.28–1.21).

To determine if the constriction amplitude and PIPR variability differed by condition, CV were calculated. The CVs ranged from 0.017 to 0.154 (mean 0.085, SD 0.027) for the minimum amplitude and 0.009 to 0.134 (mean 0.045, SD 0.023) for the PIPR amplitude, indicating that the minimum amplitude CV metric was 1.8 $\times$  more variable than the PIPR. The PIPR CVs were similar for both the melanopsin (0.046) and rod (0.044) preadapting fields, and were similar in magnitude to those reported elsewhere.<sup>13</sup> All CVs were under 0.2, indicating good consistency in the response metrics.<sup>13</sup>

## DISCUSSION

When normalized to the dark-adapted baseline, the PIPR amplitude increases systematically with increasing adapting field irradiance and duration (Fig. 2C). Because the PIPR amplitude is enhanced only at light levels above the observed melanopsin threshold for contributions to the human pupil control pathway<sup>13,14,20,34</sup> (Fig. 2C), this enhancement may reflect light adaptation, whereby the gain of the melanopsin phototransduction cascade is reduced to increase sensitivity at these suprathreshold irradiances, a process, which can take approximately 5 minutes in rat ipRGCs.<sup>23</sup> Thus, the largest effect of adaptation would be observed for the longest duration adapting field, compatible with our data demonstrating that PIPR amplitude increases with increasing adapting duration (Fig. 2C). When normalized to the light-adapted baseline, the PSPR amplitude follows a different trend to the PIPR: at irradiances below the threshold for melanopsin contributions to pupil control the PSPR is sustained (Fig. 2F), similar to the (dark adapted) PIPR in response to suprathreshold light stimulation (Fig. 2C). With increasing prestimulus adapting light irradiance, the PSPR amplitude becomes more attenuated and returns to baseline at the highest irradiances such that it's entirely suppressed (Figs. 2D, 2F). We infer from the irradiance range of this attenuation that the short-term adaptation effect on the PSPR involves a melanopsin-dependent process, consistent with the electrophysiologically measured spike frequency of melanopsin, which increases from 12 log photons $\cdot \text{cm}^{-2} \cdot \text{s}^{-1}$  with increasing irradiance.<sup>3</sup> Although systematic attenuation of the PIPR has not been previously observed, it is known that with increasing duration of a stimulus pulse with high-melanopsin excitation, the PIPR becomes less sustained.<sup>13,20,35</sup>

Together the PIPR and PSPR indicate differential effects of melanopsin adaptation on pupil control. When the pupil diameter is referenced to the dark-adapted baseline (Fig. 2A), constriction (Fig. 2B) and PIPR (Fig. 2C) amplitudes increase as the duration and irradiance of the light adaptation exposure increases. When referenced to the light-adapted baseline (Fig. 2D), increasing the irradiance of the light adaptation reduces both the constriction (Fig. 2E) and PSPR amplitudes (Fig. 2F) but increasing the duration of light adaptation (from 5–60 seconds) increases the constriction and PSPR amplitudes (Figs. 2D–F). These observations are important for the clinical measurement of melanopsin function under dark- and light-adapted conditions. The dark-adapted PIPR amplitude decreases in many retinal diseases (for review, see Feigl and Zele<sup>36</sup>). The expected pattern of change in disease will be different for

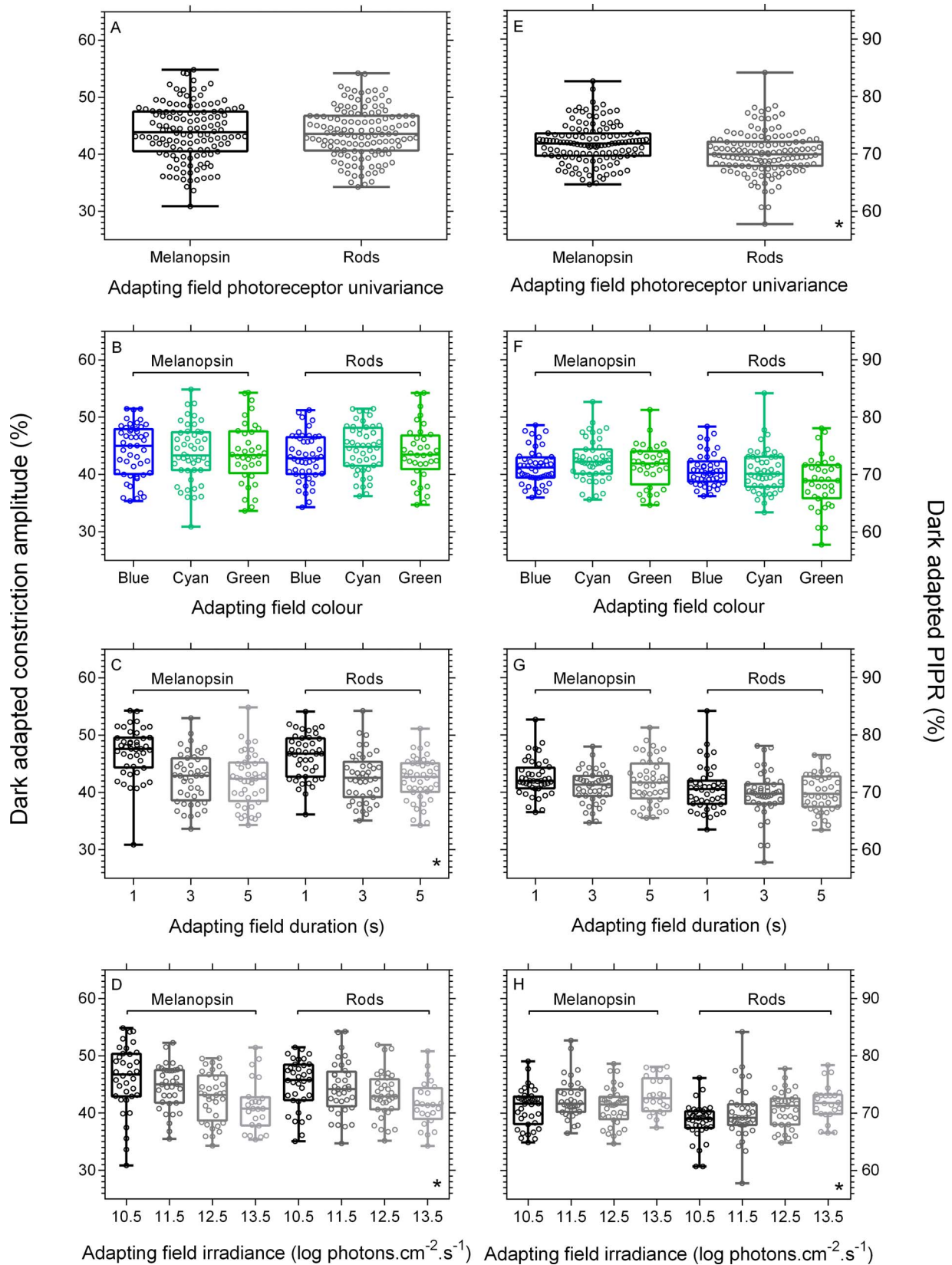


**FIGURE 5.** Effect of background field on constriction and PIPR amplitudes ( $n = 4$ ). *Left panels* depict constriction amplitude and *right panels* depict PIPR amplitude. Photoreceptor univariance data for all conditions are shown (A, B). Fields were generated to be invariant for melanopsin (*left half* of each panel) or rods (*right half* of each panel) for three colored fields (*blue, cyan, green*, [B, F]), three durations (1–5 seconds, [C, G]), and four irradiances (10.5–13.5 log photons. $\text{cm}^{-2}.\text{s}^{-1}$  [D, H]). *Plots* show 25<sup>th</sup>, 50<sup>th</sup>, and 75<sup>th</sup> percentiles and *whiskers* indicate the range. The *asterisk* in the lower right corner of a panel denotes a significant effect ( $P < 0.05$ ).

the light-adapted PSPR amplitude, depending on whether the adaptation level is above or below melanopsin threshold. It follows from our data that in individuals with ipRGC dysfunction, the PSPR amplitude will decrease (compared with healthy controls) when measured in the presence of subthreshold adapting irradiances and increase when measured in the presence of suprathreshold adapting irradiances. Further research is required to evaluate the spectral sensitivity of the light-adapted PSPR metric, to determine its photoreceptor contributions. Although the irradiance range is compatible with the PSPR being controlled by melanopsin, the role of rod<sup>15,24,37</sup> and S-cone<sup>3,38,39,40</sup> inputs to the pupil control pathway need to be considered.

The measured constriction and PIPR amplitudes are dependent on the (absolute) millimeter baseline diameter (Fig. 4). For constriction amplitude, the relationship to baseline diameter has significant clinical implications: a 1-mm increase in baseline pupil diameter increases the constriction amplitude by 1.08 mm, while the PIPR amplitude increases by 0.18 mm. Additionally, 36% of the variance in PIPR amplitude is determined by the preceding constriction amplitude. These findings demonstrate that the true stimulus effect upon the pupil response may be conflated with baseline diameter when expressed in millimeter terms. Normalizing the metrics to the baseline diameter nullifies these relationships and the constriction and PIPR amplitudes become entirely independent of baseline, allowing the true effect of the stimulus properties to be assessed. Importantly, when normalized, the constriction amplitude accounts for less than 3% of the variance in the proceeding normalized PIPR amplitude, thereby minimizing the influence of the initial constriction response to the stimulus upon the PIPR. To limit any potential effects due to individual differences in baseline pupil diameter, we recommend that pupil metrics are normalized to baseline.

Characterization of the effect of the short-term prestimulus adaptation on the dark-adapted pupil response demonstrated that increasing preadaptation duration increased the pupil constriction amplitude (Fig. 5C), but not the PIPR amplitude (Fig. 5G), which decreased with increasing adapting field irradiance (Fig. 5H). The rod adapting field univariance condition caused small (1.7%) but statistically significant increases in the PIPR amplitude when compared with the melanopsin adapting field univariance condition (Fig. 5E). That the PIPR is influenced by short-term exposure to prestimulus adapting fields independent of their duration supports the proposal that extrinsic photoreceptor inputs to ipRGCs can influence the response amplitude of the intrinsic signal<sup>22,41</sup>; potentially due to changes in membrane conduction, calcium influx, or metabotropic receptor interactions in the phototransduction cascade<sup>22</sup>; but that these small prestimulus effects on the PIPR amplitude are unlikely to be important in clinical studies. There was no effect of adapting field color upon either constriction or PIPR amplitudes, consistent with the irradiance manipulations maintaining univariance.

In conclusion, we demonstrate that short-term light adaptation presented pre- and poststimulus to a melanopsin stimulus can significantly alter the pupil constriction and PIPR amplitudes. The light adapted PIPR analogue, the PSPR, is attenuated at light levels suprathreshold for melanopsin signaling, unlike the dark-adapted PIPR, which is enhanced. We also show that normalizing the pupil metric diameters to baseline minimizes their interdependence, and that the dark adapted pupil metrics are dependent upon the photoreceptor univariance and irradiance properties of brief prestimulus fields. These findings highlight the importance of standardizing the adaptation state of participants for pupillometry in clinical practice settings.

## Acknowledgments

The authors thank Aaron A'brook for technical assistance.

Supported by grants from the Australian Research Council Discovery Projects ARC-DP140100333 (Canberra, ACT, Australia) and an Institute of Health and Biomedical Innovation Vision and Eye Program Grant (Brisbane, QLD, Australia).

Disclosure: **D.S. Joyce**, None; **B. Feigl**, None; **A.J. Zele**, None

## References

- Hattar S, Kumar M, Park A, et al. Central projections of melanopsin-expressing retinal ganglion cells in the mouse. *J Comp Neurol*. 2006;497:326–349.
- Hannibal J, Kankipati L, Strang CE, Peterson BB, Dacey D, Gamlin PD. Central projections of intrinsically photosensitive retinal ganglion cells in the macaque monkey. *J Comp Neurol*. 2014;522:2231–2248.
- Dacey DM, Liao HW, Peterson BB, et al. Melanopsin-expressing ganglion cells in primate retina signal colour and irradiance and project to the LGN. *Nature*. 2005;433:749–754.
- Berson DM, Dunn FA, Takao M. Phototransduction by retinal ganglion cells that set the circadian clock. *Science*. 2002;295:1070–1073.
- Hattar S, Liao H-W, Takao M, Berson DM, Yau K-W. Melanopsin-containing retinal ganglion cells: architecture projections, and intrinsic photosensitivity. *Science*. 2002;295:1065–1070.
- Provencio I, Jiang G, De Grip WJ, Hayes WP, Rollag MD. Melanopsin: an opsin in melanophores, brain, and eye. *Proc Natl Acad Sci U S A*. 1998;95:340–345.
- Gooley JJ, Lu J, Chou TC, Scammell TE, Saper CB. Melanopsin in cells of origin of the retinohypothalamic tract. *Nat Neurosci*. 2001;4:1165–1165.
- Do MTH, Kang SH, Xue T, et al. Photon capture and signalling by melanopsin retinal ganglion cells. *Nature*. 2009;457:281–287.
- Baver SB, Pickard GE, Sollars PJ, Pickard GE. Two types of melanopsin retinal ganglion cell differentially innervate the hypothalamic suprachiasmatic nucleus and the olivary pretectal nucleus. *Eur J Neurosci*. 2008;27:1763–1770.
- Jusuf PR, Lee SCS, Hannibal J, Grünert U. Characterization and synaptic connectivity of melanopsin-containing ganglion cells in the primate retina. *Eur J Neurosci*. 2007;26:2906–2921.
- Liao H-W, Ren X, Peterson BB, et al. Melanopsin-expressing ganglion cells on macaque and human retinas form two morphologically distinct populations. *J Comp Neurol*. 2016;1–28.
- Markwell EL, Feigl B, Zele AJ. Intrinsically photosensitive melanopsin retinal ganglion cell contributions to the pupillary light reflex and circadian rhythm. *Clin Exp Optom*. 2010;93:137–149.
- Adhikari P, Zele AJ, Feigl B. The post-illumination pupil response (PIPR). *Invest Ophthalmol Vis Sci*. 2015;56:3838–3849.
- Gamlin PDR, McDougal DH, Pokorny J, Smith VC, Yau KW, Dacey DM. Human and macaque pupil responses driven by melanopsin-containing retinal ganglion cells. *Vision Res*. 2007;47:946–954.
- Adhikari P, Feigl B, Zele AJ. Rhodopsin and melanopsin contributions to the early redilation phase of the post-illumination pupil response (PIPR). *PLoS One*. 2016;11:e0161175.
- Mure IS, Cornut PL, Rieux C, et al. Melanopsin bistability: A fly's eye technology in the human retina. *PLoS One*. 2009;4:e5991.
- Hansen MS, Sander B, Kawasaki A, Brøndsted AE, Nissen C, Lund-Andersen H. Prior light exposure enhances the pupil



- response to subsequent short wavelength (blue) light. *J Clin Exp Ophthalmol*. 2011;2:1000152.
18. Wang B, Shen C, Zhang L, et al. Dark adaptation-induced changes in rod, cone and intrinsically photosensitive retinal ganglion cell (ipRGC) sensitivity differentially affect the pupil light response (PLR). *Graefes Arch Clin Exp Ophthalmol*. 2015;253:1997-2005.
  19. Park JC, McAnany JJ. Effect of stimulus size and luminance on the rod-cone-, and melanopsin-mediated pupillary light reflex. *J Vis*. 2015;15(3):13.
  20. Park JC, Moura AL, Raza AS, Rhee DW, Kardon RH, Hood DC. Toward a clinical protocol for assessing rod cone, and melanopsin contributions to the human pupil response. *Invest Ophthalmol Vis Sci*. 2011;52:6624-6635.
  21. Wong KY. A retinal ganglion cell that can signal irradiance continuously for 10 hours. *J Neurosci*. 2012;32:11478-11485.
  22. Wong KY, Dunn FA, Graham DM, Berson DM. Synaptic influences on rat ganglion-cell photoreceptors. *J Physiol*. 2007;582:279-296.
  23. Wong KY, Dunn FA, Berson DM. Photoreceptor adaptation in intrinsically photosensitive retinal ganglion cells. *Neuron*. 2005;48:1001-1010.
  24. McDougal DH, Gamlin PD. The influence of intrinsically-photosensitive retinal ganglion cells on the spectral sensitivity and response dynamics of the human pupillary light reflex. *Vision Res*. 2010;50:72-87.
  25. Enezi Ja, Revell V, Brown T, Wynne J, Schlangen L, Lucas R. A "melanopic" spectral efficiency function predicts the sensitivity of melanopsin photoreceptors to polychromatic lights. *J Biol Rhythms*. 2011;26:314-323.
  26. Crawford BH. The scotopic visibility function. *Proc Phys Soc B*. 1949;62:321.
  27. Mitchell DE, Rushton WAH. The red/green pigments of normal vision. *Vision Res*. 1971;11:1045-1056.
  28. Rushton WAH. Review lecture. Pigments and signals in colour vision. *J Physiol*. 1972;220:1-31.
  29. Zele AJ, Feigl B, Smith SS, Markwell EL. The circadian response of intrinsically photosensitive retinal ganglion cells. *PLoS One*. 2011;6:e17860.
  30. Joyce DS, Feigl B, Cao D, Zele AJ. Temporal characteristics of melanopsin inputs to the human pupil light reflex. *Vision Res*. 2015;107:58-66.
  31. Kankipati L, Girkin CA, Gamlin PD. Post-illumination pupil response in subjects without ocular disease. *Invest Ophthalmol Vis Sci*. 2010;51:2764-2769.
  32. Herbst K, Sander B, Milea D, Lund-Andersen H, Kawasaki A. Test-retest repeatability of the pupil light response to blue and red light stimuli in normal human eyes using a novel pupillometer. *Front Neurol*. 2011;2.
  33. Wilhelm H, Wilhelm B. Clinical applications of pupillography. *J Neuroophthalmol*. 2003;23:42-49.
  34. Lei S, Goltz HC, Chandrakumar M, Wong AMF. Full-field chromatic pupillometry for the assessment of the postillumination pupil response driven by melanopsin-containing retinal ganglion cells. *Invest Ophthalmol Vis Sci*. 2014;55:4496-4503.
  35. Münch M, Léon L, Crippa SV, Kawasaki A. Circadian and wake-dependent effects on the pupil light reflex in response to narrow-bandwidth light pulses. *Invest Ophthalmol Vis Sci*. 2012;53:4546-4555.
  36. Feigl B, Zele AJ. Melanopsin-expressing intrinsically photosensitive retinal ganglion cells in retinal disease. *Optom Vis Sci*. 2014;91:894-903.
  37. Barrionuevo PA, Nicandro N, McAnany JJ, Zele AJ, Gamlin P, Cao D. Assessing rod, cone and melanopsin contributions to human pupil flicker responses. *Invest Ophthalmol Vis Sci*. 2014;55:719-727.
  38. Spitschan M, Jain S, Brainard DH, Aguirre GK. Opponent melanopsin and S-cone signals in the human pupillary light response. *Proc Natl Acad Sci U S A*. 2014;111:15568-15572.
  39. Allen AE, Brown TM, Lucas RJ. A distinct contribution of short-wavelength-sensitive cones to light-evoked activity in the mouse pretectal olivary nucleus. *J Neurosci*. 2011;31:16833-16843.
  40. Cao D, Nicandro N, Barrionuevo PA. A five-primary photostimulator suitable for studying intrinsically photosensitive retinal ganglion cell functions in humans. *J Vis*. 2015;15(1):27.
  41. Belenky MA, Smeraski CA, Provencio I, Sollars PJ, Pickard GE. Melanopsin retinal ganglion cells receive bipolar and amacrine cell synapses. *J Comp Neurol*. 2003;460:380-393.